PNAS
www.pnas.org

Supplementary Information for

Species-specific mechanisms of cytotoxicity toward immune cells determine the successful outcome of *Vibrio* infections

Tristan Rubio[a*], Daniel Oyanedel-Trigo[a*], Yannick Labreuche[b,c], Eve Toulza[a], Xing Luo[d], Maxime Bruto[b,c], Cristian Chaparro[a], Marta Torres[a,d,e], Julien de Lorgeril[a], Philippe Haffner[a], Jeremie Vidal-Dupiol[a], Arnaud Lagorce[a], Bruno Petton[b], Guillaume Mitta[a], Annick Jacq[d], Frédérique Le Roux[b,c], Guillaume Charrière[a] and Delphine Destoumieux-Garzón[a]

Delphine Destoumieux-Garzón. ddestoum@ifremer.fr
Guillaume Charrière. guillaume.charriere@umontpellier.fr
Frédérique Le Roux. frederique.le-roux@sb-roscoff.fr

This PDF file includes:

Supplementary text
Figs S1 to S13
Tables S1 to S4
References for SI reference citations

www.pnas.org/cgi/doi/10.1073/pnas.1905747116

Supplementary text. Materials and Methods

References for SI reference citations

Supplementary Information Text

Materials and Methods

Strains, plasmids, and primers

Virulent strains used in this study were *V. tasmaniensis* LGP32 (1), *V. crassostreae* J2-9 (2). Non-virulent strains were *Vibrio sp.nov.* J2-8, close phylogenetic neighbor of the virulent *V. crassostreae* population (2) as well as the type strain of *V. tasmaniensis* LMG20 012T (3). Other strains, plasmids and primers used or constructed in the present study are described in SI Appendix Tables S2-S3-S4.

Animals

C. gigas diploid oyster spat were used from three families of siblings (referred to as Decipher #1, #14 and #15) (4) and a batch of standardized Ifremer spats (NSI) were produced from a pool of 120 genitors (5). Animals were from both sexes. Spats (4 to 6 months old) were used for experimental infections and dual RNA-seq. Adults (18 months old) produced from a pool of 120 genitors (ASI) were used to collect hemolymph for cytotoxicity assays. All oysters were produced at the Ifremer hatchery in Argenton, France. All families have been tested in experimental infections. The oysters of family #14 were chosen for the RNA-seq experiments.

Experimental infections

Experimental infections were performed at 20 °C by adapting a previously described procedure (6). Briefly, oysters were anesthetized for 3 h (7). Groups of 20 juvenile oysters (1.5-2 cm) were then distributed into tanks containing 3 L of seawater, per condition. Stationary phase cultures of bacteria (20 h at 20 °C) were washed by centrifugation (15 min, 1500 g, 20 °C) and resuspended in sterile seawater (SSW) before injecting at 7.5×10^7 CFU into oyster adductor muscle. Mortalities were monitored daily for 7 days. Two tanks were monitored per condition. Statistical analyses were performed using non-parametric Kaplan Meier test in order to estimate log-rank values for comparing conditions (GraphPad Prism 6). All experimental infections were performed according to the Ifremer animal care guidelines and policy.

Molecular microbiology

Vibrio isolates were grown at 20 °C in Zobell broth or agar (4 $g.l^{-1}$ bactopeptone and 1 $g.l^{-1}$ yeast extract in artificial seawater, pH 7.6), Luria-Bertani (LB) broth or LB-agar (LBA) containing 0.5 M NaCl. *Escherichia coli* strains were grown at 37°C in LB or on LBA for cloning and conjugation experiments. Chloramphenicol (Cm, 5, 10 or 25$\mu g.ml^{-1}$ depending on the strain), thymidine (0.3 mM) and diaminopimelate (0.3 mM) were added as supplements when necessary. Conjugation between *E. coli* and *Vibrio* were performed at 30 °C as described previously (8). To label the strains with a fluorochrome, *gfp* gene was cloned in Apa1/Xho1 sites of the pMRB plasmid known to be stable in *Vibrio spp.* (9) resulting in a constitutive expression from a P_{lac} promoter. Gene inactivation was performed by cloning about 500 bp of the target

gene in pSW23T (10) and selecting on Cm the suicide plasmid integration obtained by a single recombination (11). Mutants were screened for insertion of the suicide vector by PCR using external primers flanking the different targeted genes.

Histology

Groups of 10 spats (1.5-2 cm) were injected with 7.5 x 10^7 CFU of GFP-expressing LGP32 or J2-9. Groups of 5 spats were injected with 7.5 x 10^7 CFU of GFP-expressing LMG20 012T or J2-8 (controls). Two non-injected oysters were used as controls. Spats were distributed in one tank containing 3 L of seawater per condition, at 20 °C. Oysters were sampled and fixed 8 h after injection, in seawater Davidson (20% of formaldehyde, 30% of sterile seawater, 10% of glycerol and 30% of 95% ethanol). Histological sectioning was performed at HISTALIM, Montpellier, France. Briefly, oysters were extracted from the shell, tissues were dehydrated and included in paraffin with an inclusion automaton. Longitudinal sections were immunostained with an anti-GFP primary antibody coupled to alkaline phosphatase (Abcam). Revelation was performed with the PA-Red kit (Roche). Sections were scanned with slide scanner Hamamatsu NANOZOOMER. Hemocytes were observed with the ZEISS Z1 microscope equipped with Zeiss 63X/1.4 Plan-Apo Oil objective.

In vitro cytotoxicity assays

Hemocytes were plated in 96 well-plates (2 x 10^5 cells/well) or in 12 well-plates (5 x 10^5 cells/well) with a Transwell Permeable Support with a pore size of 0.4 µm. After 1 h, plasma was removed and 5 µg/µl Sytox Green (Molecular Probes) diluted in 200µl sterile seawater was added to each well. Vibrios, previously washed and opsonized in plasma for 1 h, were then added to the wells at a MOI of 50:1. Sytox fluorescence was monitored (λ_{ex} 480nm/λ_{em} 550nm) for 15 h using a TECAN microplate reader. Maximum cytolysis was determined by adding 0.1% Triton X-100 to hemocytes. To determine the role of phagocytosis in the vibrio-induced cytolysis of hemocytes, 5 µg/ml cytochalasin D was added to the wells 30 min before addition of vibrios. Statistical analysis was performed using RM-ANOVA.

Confocal microscopy of interaction between hemocytes and vibrios *in vivo*

Groups of 15 juvenile oysters (4-5 cm) were injected with 1.5 x 10^8 CFU of GFP-expressing vibrios (either J2-8 or J2-9) *a priori* washed and resuspended in sterile seawater. Control oysters received an injection of an equal volume of sterile seawater. For each experimental condition, hemolymph was collected from five oysters at 2 h, 4 h and 8 h after injection. Samples were fixed with 4% paraformaldehyde for 15 min and cytospun at 600 g for 10 min onto Superfrost glass slide. Glass slides were then washed with PBS and stained with 0.25 µg/ml DAPI (Sigma) and 1 µg/ml Phalloïdine-TRITC (Sigma) for 30 min at room temperature. Microscopy was performed using Leica DM 2500 confocal microscope with a Leica 63x ACS APO 1.3 objective.

Dual RNA-seq experiments

Three independent experimental infections were performed on juvenile oysters from family Decipher#14 as described above. For every independent experiment, 150 oysters (30 animals per condition) were injected with either bacteria (10^7 CFUs of LGP32, LMG20012T, J2-9, J2-8 overnight cultures washed in sterile seawater), or sterile seawater (mock-infected oysters). In addition, both bacterial suspensions and 30 non-treated oysters were collected at time 0. For every experimental condition, 30 oysters were then sampled 8 h after injection (*i.e.* before mortality occurred). Oysters were extracted from shell and immediately frozen in liquid

nitrogen. Pools of tissues from 30 oysters were ground by bead-beating (Retsch, Mixer Mill MM400) with a stainless-steel ball pre-chilled in liquid nitrogen. Both, oyster powder homogenates and bacterial suspensions, were lysed in 1.6 ml Trizol (Life technologies Inc.) and vortexed for 2.5 h at 4 °C. Samples were then stored at -80 °C until RNA extraction.

RNA was extracted from oyster tissues using the Direct-Zol RNA Miniprep kit from Proteigene, and according to the manufacturer's protocol. RNA concentration and purity were checked with a Nanodrop ND-1000 spectrometer (Thermo Scientific, Les Ulis, France; oyster RNA-seq) or a DS-11 Spectrophotometer (DeNovix Inc.; bacterial RNA-seq) and the integrity of the RNA was analyzed by capillary electrophoresis with an Agilent BioAnalyzer 2100. For oyster RNA-seq, library construction and sequencing were performed on polyadenylated mRNAs by the Fasteris Company (Switzerland, https://www.fasteris.com). Directional cDNA libraries were constructed and sequenced on an Illumina Hiseq, in paired-end reads of 2 x75 bp. For bacterial RNA-seq, total RNA obtained from oyster tissues was used to prepare non rRNA-bacterial RNA enriched libraries. After polyadenylated mRNAs (i.e. host mRNAs) were removed using MICROB*Enrich*™ Kit (Ambion), cDNA oriented sequencing libraries were prepared starting from 100 ng enriched RNA using Ovation Universal RNA-Seq System kit (NuGEN). Library construction included a depletion step of abundant, non-desired sequences, using a Nugen-customized mixture of primers complementary to RNA sequences to be depleted, viz. oyster nuclear, mitochondrial, and ribosomal and bacterial ribosomal RNA sequences. The libraries were quantified by DeNovix dsDNA Broad Range Assay (DeNovix Inc.) and the quality was monitored using Agilent High Sensitivity DNA kit (Agilent Technologies). For each condition, three biological replicate libraries were prepared. Libraries were sequenced in paired-end mode (2 × 150 bp) by Fasteris on an Illumina HiSeq 4000, to obtain ~ 100 million reads per sample/per run.

Oyster transcriptome analysis

For oyster RNA-seq data, data treatment was carried out using the galaxy instance of the IHPE lab (https://bioinfo.univ-perp.fr) (12). Phred quality scores were checked using the FastX toolkit galaxy interface (http://hannonlab.cshl.edu/fastx_toolkit/) and were higher than 26 for over 90% of the read length for all the sequences. All the reads were thus kept for subsequent analyses. Mapping to the *C. gigas* reference genome (assembly version V9 (13)) was performed using RNAstar (Galaxy Version 2.4.0d-2, (14)). HTSeq-count was used to count the number of reads overlapping annotated genes (mode Union) (Galaxy Version v0.6.1) (15). The resulting files were used as input to determine differential expression for each feature between oysters injected with vibrios and mock-infected oysters using DESeq2 (16). Fold changes in gene expression between test animals and controls were considered significant when the adjusted *P*-value (P_{adj}) for multiple testing with the Benjamini-Hochberg procedure, which controls false discovery rate (FDR), was < 0.05. The same threshold was applied to fold changes in gene expression between mock-infected oysters and naïve controls. Oyster RNA-seq

data has been made available through the SRA database (BioProject accession number PRJNA515169) under SRA accessions SRR8551076-SRR8551093.

As genes for *C. gigas* antimicrobial peptides (AMPs) are not annotated in the *C. gigas* reference genome (assembly version V9, (13)), read counts for all AMPs were obtained by alignment to an in-house database of AMP protein sequences using DIAMOND 0.7.9 (17). The AMPs database was prepared using diamond 'makedb' and the reads for each sample/replicate were compared to the database using diamond 'blastx'. Alignments were filtered for the best hit and e-value < 1e-6. Read counts for each AMP were normalized against the total sequence number for each sample/replicate.

Vibrio transcriptome analysis

For bacterial RNA-seq data, all the analyses but the last step (DESeq2) were carried out on a personal computer (Ubuntu 16.04 LTS), on which the necessary tools were executed from a docker container image (https://www.docker.com/why-docker). Raw Illumina® sequencing reads were trimmed by Trimmomatic in paired-end mode (18) to remove sequences corresponding to the NuGen provided adapters, clipping part of reads having a quality score of below 20, and dropping reads of less than 36 nt. The two resulting files containing the forward and reverse reads, respectively, of the paired-end reads, were used as input for Bowtie2 (19) to align the reads on *V. tasmaniensis* LGP32 or *V. crassostrea* J2-9 genome, respectively. In the case of LGP32, where the complete genome is available, the sequences of the two chromosomes were concatenated. In the case of J2-9, the genomic sequence corresponds to a concatenation of multiple contigs. In addition, whereas the rRNA operon was present in multiple copies in the genome of LGP32, it was unique in the J2-9 sequence file. We thus artificially duplicated the operon sequence in J2-9 so that reads corresponding to rRNA genes were listed by Bowtie2 as those with multiple alignments, and thus were eliminated as it was the case for LGP32.

As expected, in the case of bacterial RNA-seq samples resulting from oyster infection experiments, the rate of read alignment on the bacterial genome was ~2% at the most, whereas it was more than 98% in the case of the *in vitro* grown bacteria. To prevent a potential bias induced by this difference in the subsequent computational steps, we introduced a random downsampling step of the aligned reads of the control samples (*in vitro* growth). This was done using the command "downsampleSam" of the Picard tools (http://broadinstitute.github.io/picard/command-line-overview.html#DownsampleSam) with p= 0.02, leading to a number of aligned reads similar to what was obtained in case of the oyster infection samples. Counts for each annotated feature (CDS + sRNAs) of either *V. tasmaniensis* LGP32 or *V. crassostreae* J2-9 were then computed using featureCounts (20). The resulting files were used as input to determine differential expression for each feature between oyster injected with vibrios and vibrios grown *in vitro* by DESeq2 (16). DESeq2 was carried out on a Galaxy instance at the INRA migale bioinformatics platform: http://migale.jouy.inra.fr/galaxy/. Genes were considered as differentially

expressed between tested conditions and controls when |log2(fold change)| was ≥1 and adjusted *P*-value (P_{adj}) for multiple testing with the Benjamini-Hochberg procedure was < 0.05. Bacterial RNA-seq data has been made available through the SRA database: BioProject accession number PRJNA521688 under SRA accessions SRR8567597-SRR8567602 (*Vibrio crassostreae* J2-9) and BioProject accession number PRJNA521693 under SRA accessions SRR8573808- SRR8573813 (*Vibrio tasmaniensis* LGP32).

Functional gene ontology annotations

For oyster genes, Blastx (21) comparison against NR database was performed for each set of genes with a maximum number of target hits of 20 and a minimal e-value of 0.001. XML blast result files were loaded onto Blast2GO (22) for GO mapping and annotation of the B2G database. Functional categories corresponding to significantly modulated genes (331 genes), were then determined manually; this was supported by background literature review. A heatmap of the mean of log2 fold change in three independent experiments was then generated using cluster 3.0 (http://bonsai.hgc.jp/~mdehoon/ software /cluster/software.htm).

For bacterial genes, annotations of differentially expressed genes (fold change ≥ 2 and padj ≤ 0.05) were manually curated using the MicroScope platform (23) and the MetaCyc data base (24). Based on these curated annotations, each gene was assigned to one of 32 functional categories (see Figs 5 & S5 for the list of categories). In addition, with the help of the tools provided by MicroScope, which allows for comparison between genomes based on sequence and synteny conservation; we identified genes which were common to both (J2-9 and LGP32) differential transcriptomes, with the exception of genes of unknown function. This subset of genes is defined as the intersection between the J2-9 and LGP32 differential transcriptomes.

RT-qPCR

RT-qPCR was performed either on the same RNA samples as those used for deep sequencing to validate RNAseq data (Fig. S3), or on specific RNA samples in order to monitor the time-course of bacterial gene expression in oysters (Fig S6). cDNA was synthetized using M-MLV RT (Invitrogen Inc.) using 1 µg of RNA and random primers (250 ng). Real-time qPCR was performed at the qPHd platform of qPCR in Montpellier using the Light-Cycler 480 System (Roche) and oyster gene specific primers (Table S8). The total Real-time qPCR reaction volume was 1.5 µl with 0.5 µl cDNA (40 ng µl^{-1}) and 1 µl LightCycler 480 SYBR Green I Master mix (Roche) containing 0.5 µM PCR primer (Eurogentec SA). Relative expression was calculated using the $2^{-\Delta\Delta Cq}$ method (Pfaffl, 2001), with normalization to the *C. gigas* reference genes, namely, *Cg*-RPL40 (GenBank FP004478), *Cg*-RPS6 (GenBank HS119070) and *Cg*-EF1α (GenBank AB123066). For understanding the time-course of the bacterial gene expression, 6-phosphofructokinase (VS_2913) and Methyl glyoxal synthase (VS_II1055) genes (Vanhove et al., 2016) were used as reference genes to monitor the relative expression of *vipA1* and *vipA2.*

Specific vibrio quantification by qPCR

Genomic DNA was extracted with the DNA kit Promega (Wizard SV Genomic DNA Purification System) on the same oyster samples used for RNA-seq. DNA concentration was measured using a NanoDrop 1000 Spectrophotometer (Thermo Fisher Scientific Inc.). Real-time qPCR was performed on a Light-Cycler 480 System (Roche). The total Real-time qPCR reaction volume was 1.5 µl with 0.5 µl cDNA (40 ng μl^{-1}) and 1 µl LightCycler 480 SYBR Green I Master mix (Roche) containing 0.5 µM PCR primer (Eurogenetec SA). Strain-specific primers were designed using Primer 3 plus (http://primer3plus.com/), to amplify monocopy genes from specific vibrio genomes (Table S8). Efficiency and specificity were checked on DNA extracted from six different vibrio strains. To quantify oyster genomes, *Cg*-BPI (GenBank: AY165040) primers were used (Table S8). The vibrio charge in oyster tissues was calculated as a number of vibrio genome copies per number of oyster genome copy considering the following genome sizes: *C. gigas* (637 Mbp), LGP32 (4.97 Mbp), LMG20012T (4.84 Mbp), J2-9 (5.79 Mbp), J2-8 (5.39 Mbp).

Vibrio genome sequencing and assembly

Genomic DNA for the J0-13, J5-13 and J5-9 strains was extracted with the NucleoSpin Tissue kit (Macherey-Nagel Inc.). Starting from 1 ng DNA, library construction was performed at the Bio-Environnement platform (University of Perpignan, France) with the Nextera XT kit (Illumina, USA) in paired-end mode (2 × 150 bp). Sequencing was carried out using a NextSeq 550 instrument resulting in ~100-fold coverage. Reads were assembled *de novo* using Spades software. Computational prediction of coding sequences together with functional assignments was performed using the automated annotation pipeline implemented in the MicroScope platform (25). The genome sequences of *V. tasmaniensis* J0-13, J5-13 and J5-9 were deposited in Genbank with the following accession numbers: SEOP00000000, SESM00000000 and SESL00000000.

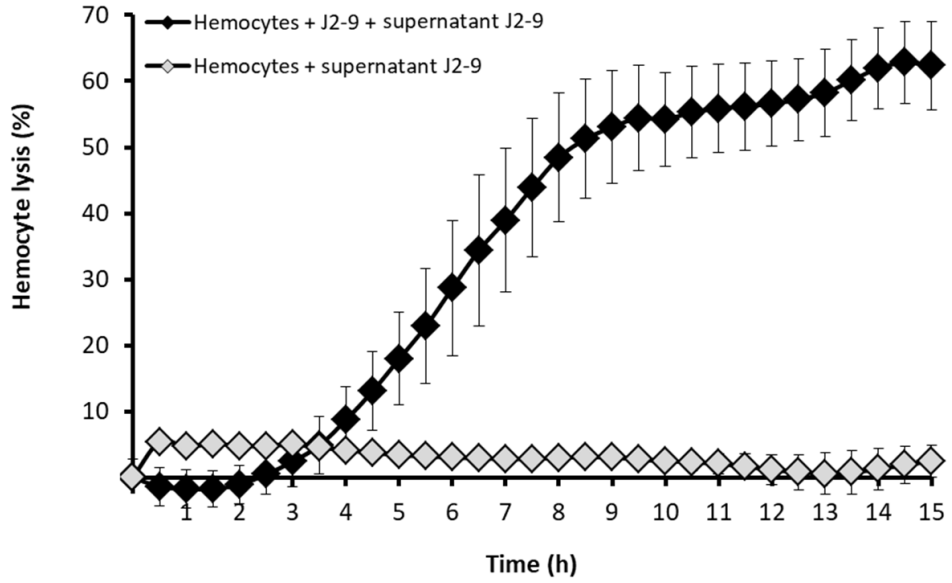

Figure S1 | Extracellular secretion products of J2-9 are not cytotoxic to hemocytes.

Cytotoxicity of J2-9 was monitored on monolayers of hemocytes by measuring the fluorescence of Sytox green over 15 hours. At time 0, J2-9 cells (overnight culture) were added to hemocyte monolayers at a MOI of 50:1. Alternatively, an overnight culture supernatant of J2-9 devoid of bacteria (secretion products only) was added to hemocytes. The graph shows the time course of cytotoxicity of J2-9 (black diamonds) and the lack of cytotoxocity of J2-9 secretion products (grey diamonds). The error bars represent the standard deviation of technical triplicates. Data are representative of three independent experiments.

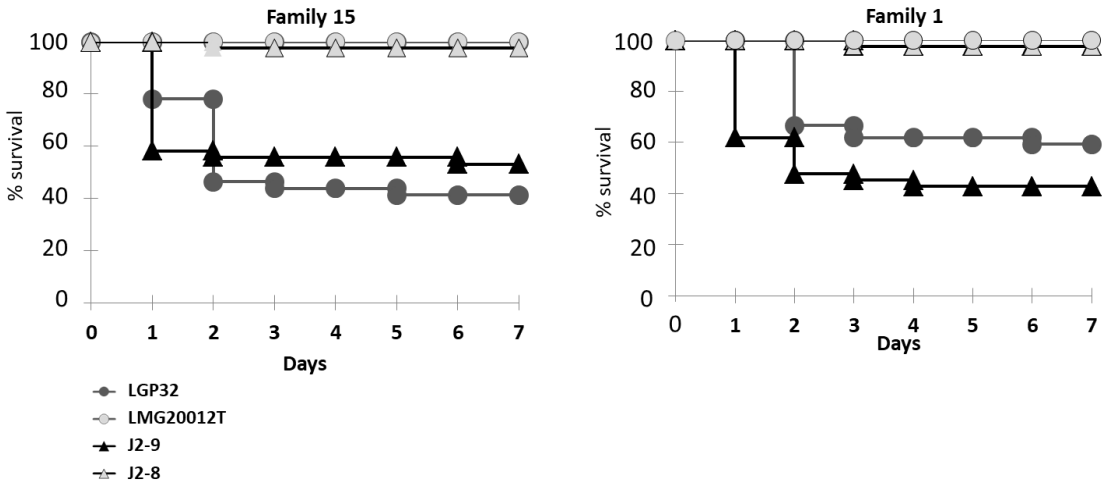

Figure S2 | Virulence of *V. tasmanienis* LGP32 and *V. crassotreae* J2-9 is independent on oyster genetic background.

Kaplan Meier survival curves were generated from two additional families of biparental oysters injected with 7.5 x 10^7 CFU per oyster of LGP32, J2-9, LMG20012T or J2-8. Mortalities were monitored on 2 groups of 20 oysters per family (2 seawater tanks per condition) during 7 days after injection.
(A) Mortalities on oyster Decipher family #15. LGP32, J2-9 and J2-8 induced 58.7%, 46% and 2.3% of mortalities of oysters respectively. LMG20012T did not induce mortalities. J2-9 and LGP32 conditions are not significantly different (Log-rank p-value=0.560).
(B) Mortalities on oyster Decipher family #1. LGP32, J2-9 and J2-8 induced 40.7%, 57.1% and 3.3% of mortalities in oysters, respectively. LMG20012T did not induce mortalities. J2-9 and LGP32 conditions are not significantly different (Log-rank p-value=0.401).

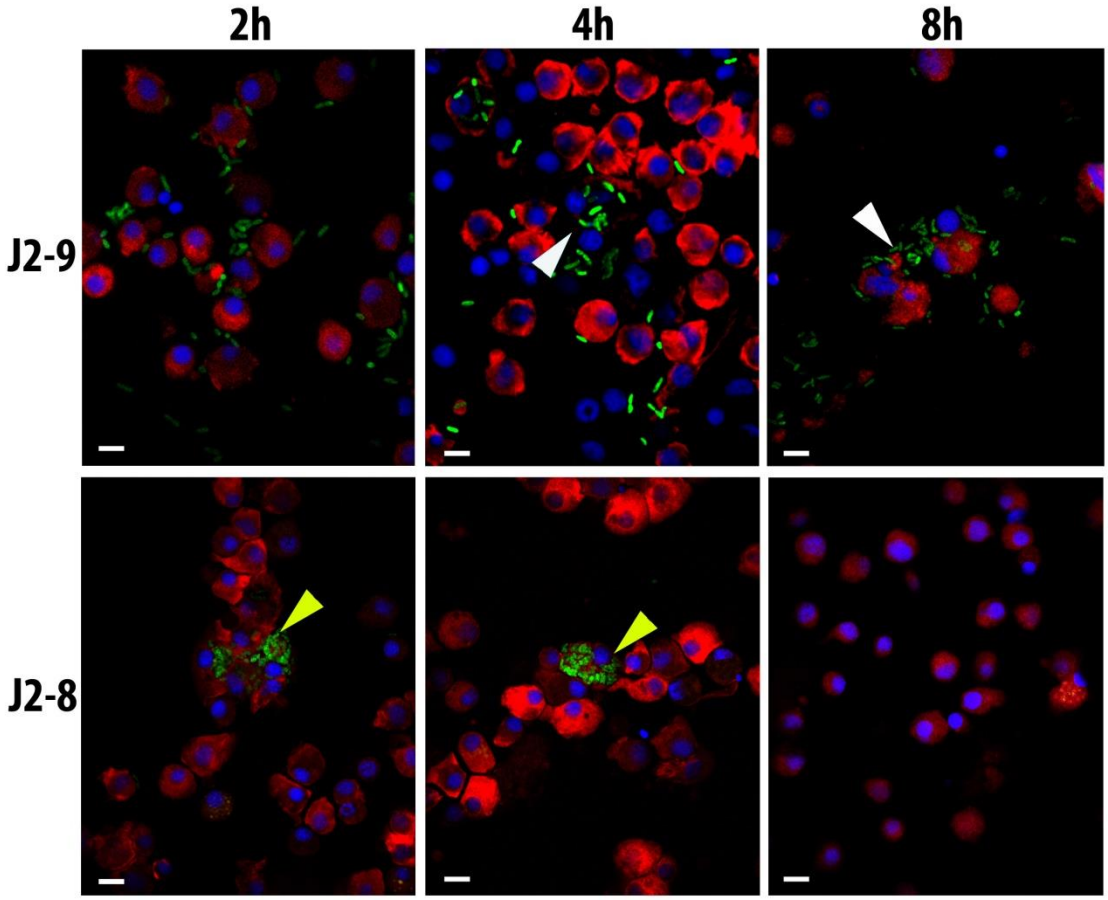

Figure S3 | Only non-virulent vibrios are degraded by hemocyte phagocytosis

Confocal microscopy of hemolymph collected from animals infected with *V. crassostrea* J2-9 or the non-virulent control J2-8. Juvenile oysters were injected with 1.5 x 10^8 CFU of GFP-expressing vibrios. For each experimental condition, hemolymph was withdrawn from five oysters, at 2, 4, and 8 h after injection. Hemocytes were observed by confocal microscopy on cytospin glass slides after the staining of nuclei and actin cytoskeleton with DAPI and phalloidin-TRITC, respectively. In oysters injected with J2-9, J2-9 cells were mostly extracellular and were detected at every time-point (white arrows). In contrast, the non-virulent J2-8 was massively phagocytized (yellow arrows) as soon as 2 h after infections showing loss of cell interatity at 4 h; they became almost undetectable after 8h in the oyster hemolymph. Scale bar: 10 µm.

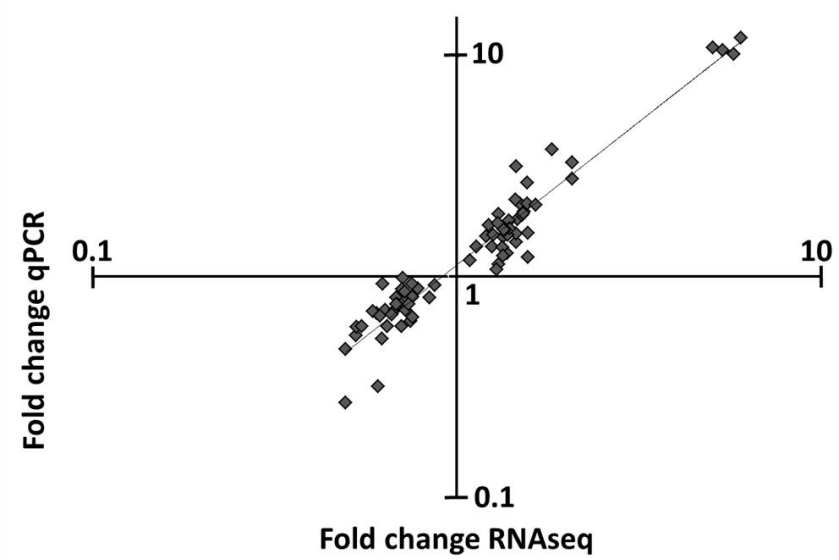

Figure S4 | Validation of the RNAseq data using quantitative RT-PCR.

Nineteen oyster genes were selected and their expression (relative to the control genes *ef1, c23* and *RP56*) was quantified by qRT-PCR in RNA samples used for each RNAseq condition. Expression data were compared to those obtained using the RNAseq approach (normalized read counts). Fold changes of RNAseq were fully validated by qPCR (R^2=0.926, $p<0.001$ linear regression test).

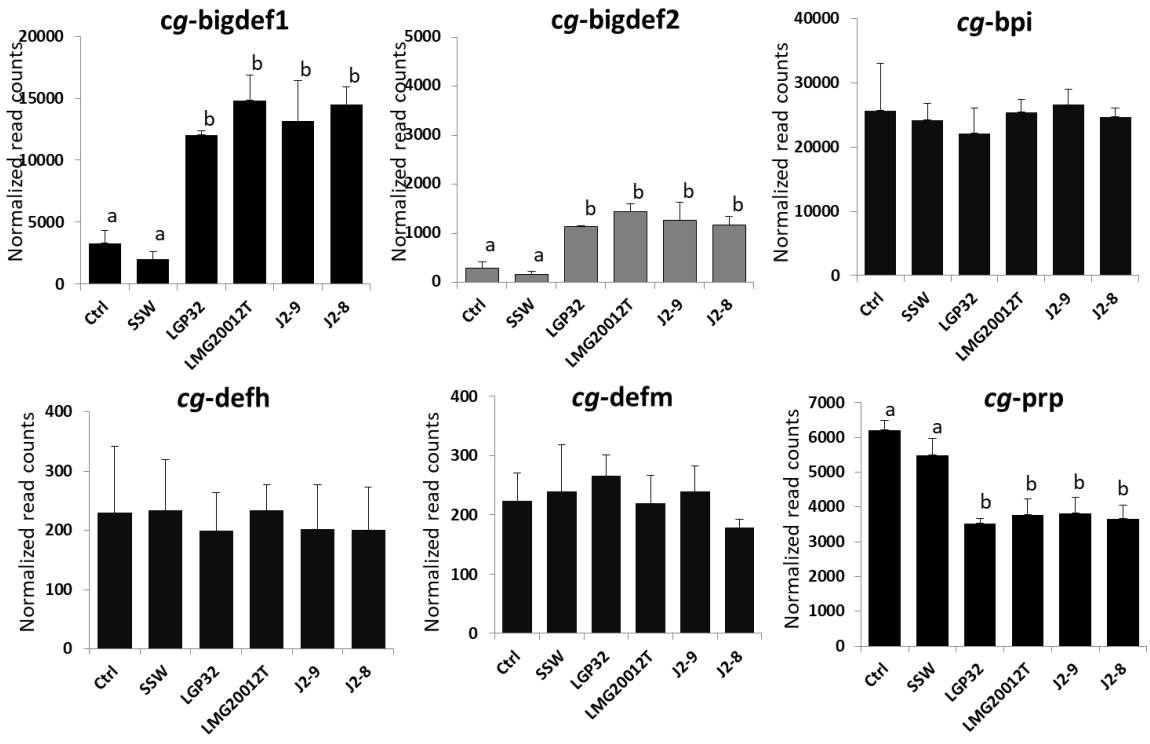

Figure S5 | Antimicrobial peptides respond similarly to virulent and non-virulent strains.

Normalized read counts for AMP genes (*cg-bigdef1, cg-bigdef2, cg-bpi, cg-defh, cg-defm, cg-prp*) are plotted for vibrio-infected oysters (LGP32, LMG20012T, J2-9,J2-8), mock-infected oysters (sterile seawater, SSW) and naive oysters (Ctrl). *cg*-bigdef3 was absent from oyster family Decipher#14. Statistical analysis was performed using One-way ANOVA ($p<0.001$)

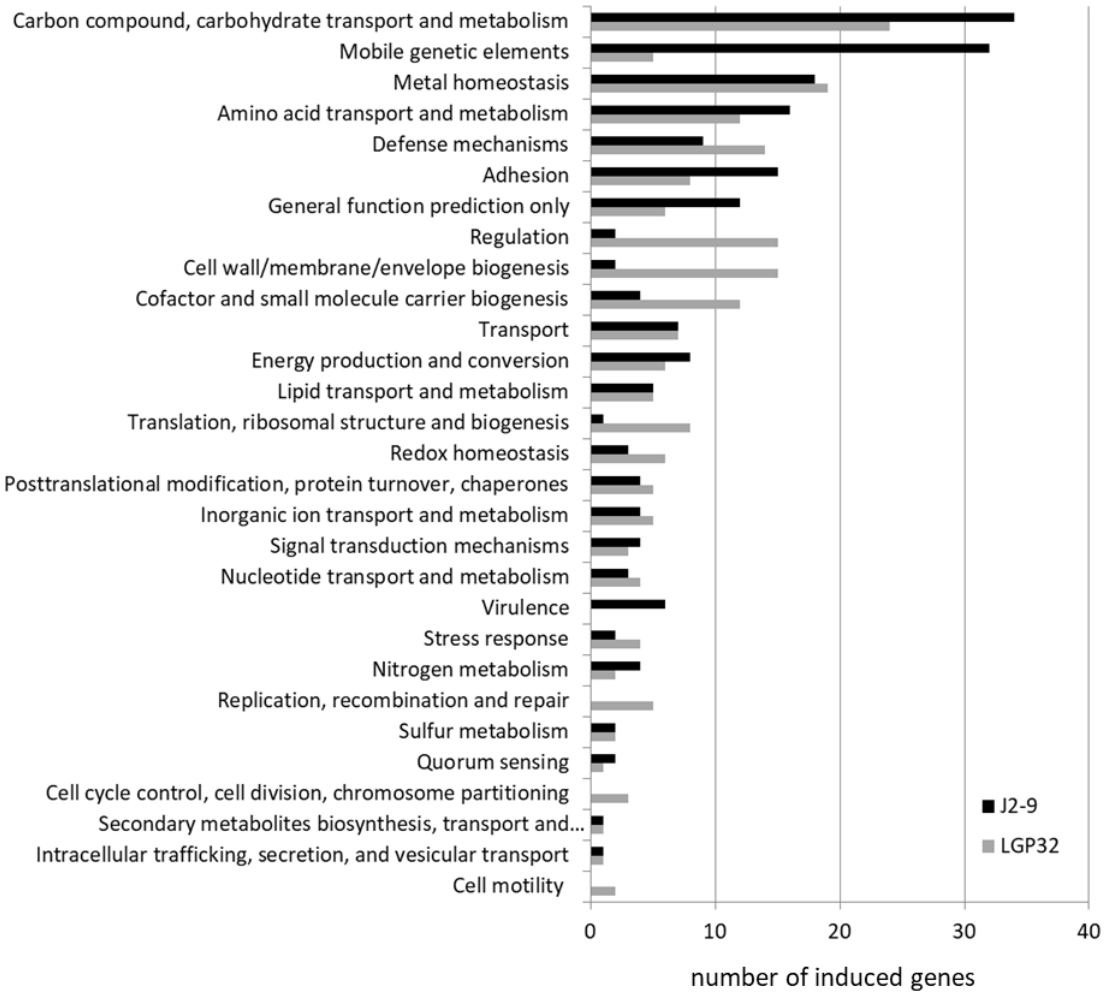

Figure S6 | Functional distribution of the 200 most induced *Vibrio* genes revealed by within host bacterial RNAseq.

LGP32 and J2-9 transcripts were sorted according to foldchanges, the 200 most-induced genes during oyster colonization were then counted according to functional categories (genes without annotated function were not included).

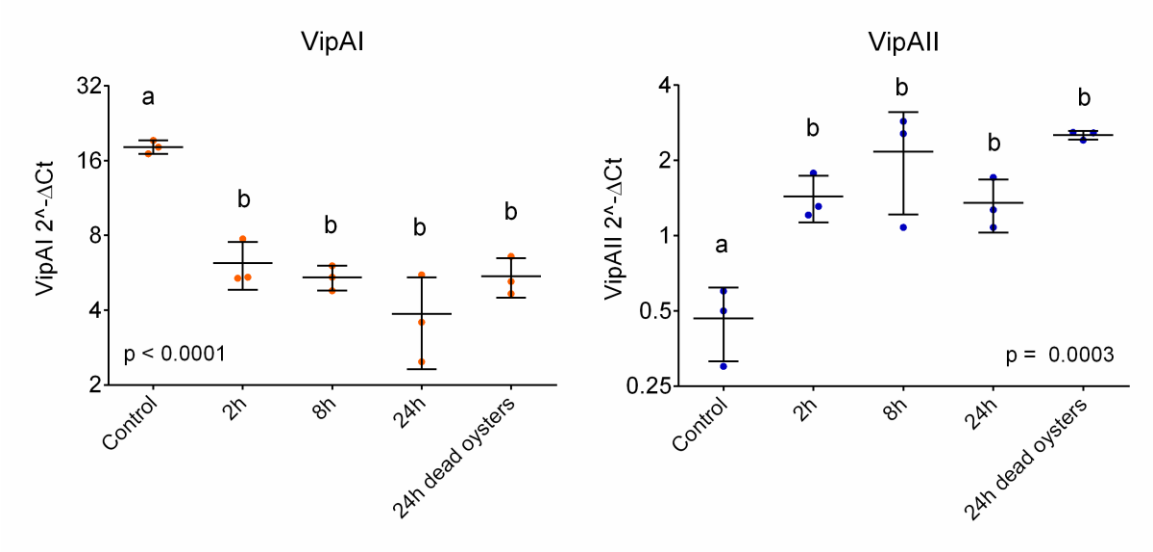

Figure S7 I qPCR monitoring of *vipA1* (VS-1332) and *vipA2* (VS_II0997) during host colonization.

An overnight culture of *V. tasmaniensis* LGP32 was washed and resuspended in sterile seawater (SSW). Part of the bacterial suspension was immediately frozen for future RNA extraction (Control). In parallel, 300 juvenile oysters (NSI produced at Ifremer Argenton) were injected with the bacterial suspension (6 x 10^7 CFU per animal, 100 animals per tank). At each time point (2h, 8h, 24h), 10 live oysters and 10 dead oysters (for 24h only) were collected from each tank. Oysters were snap frozen in liquid nitrogen and grinded for RNA extraction. *vipA1* and *vipA2* expression were compared to the geometric mean of two reference genes 6PKF (VS_2913), MGS (VS_II1055). Data correspond to $2^{-\Delta Ct}$ values and Y-axis are in the log scale. Each dot represents a pool of 10 oysters. Data show that *vipA1* expression is frontloaded as opposed to the within-host induction of *vipA2.* Significance established by a One-way ANOVA with Tukey's multiple comparisons test.

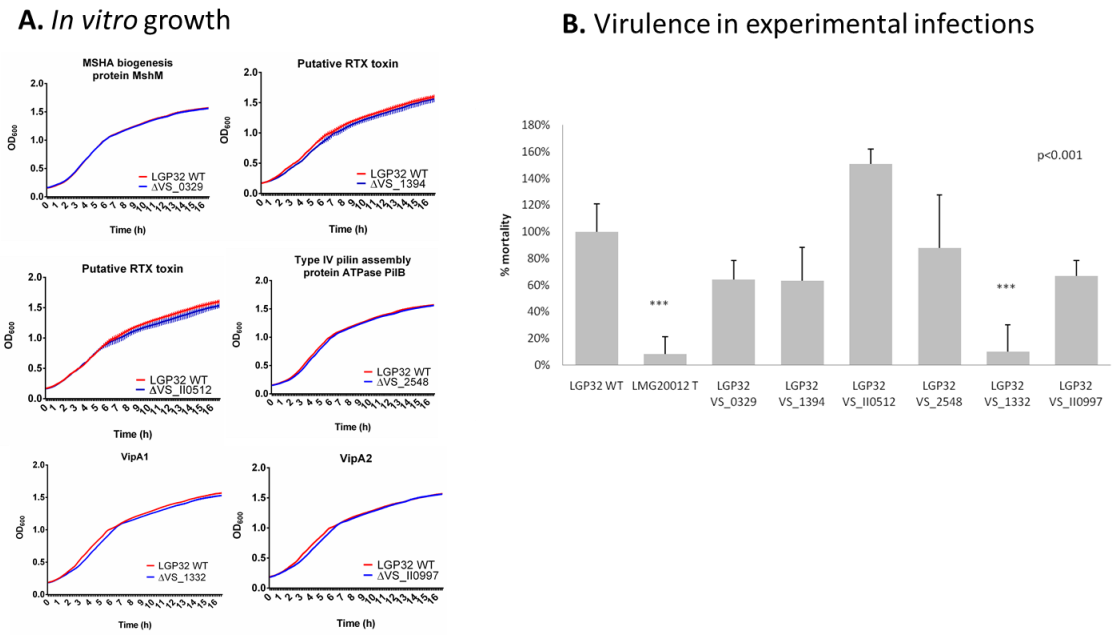

Figure S8 | Phenotyping of *V. tasmaniensis* LGP32 mutants.

A. Growth curves of wild-type LGP32 and isogenic mutants. Cultures were made in LB NaCl 0.5M. OD_{600} was recorded in triplicate for each strain every 10 minutes after continuous orbital shaking in a TECAN M200 Infinite Pro plate reader, for a 16 hour period at 20°C. B. Virulence in oyster experimental infections. Virulence was assessed by intramuscular injection of juvenile oysters in four independent experiments. LMG20012T was used as a negative control. Mortalities were recorded at day 1. Data are expressed as a percentage of the mortality induced by the wild-type strains. Strains or mutants significantly less virulent than the wild-type LGP32 are indicated by asterisks (Test Kruskal-Wallis, Dunn). ***p<0.001

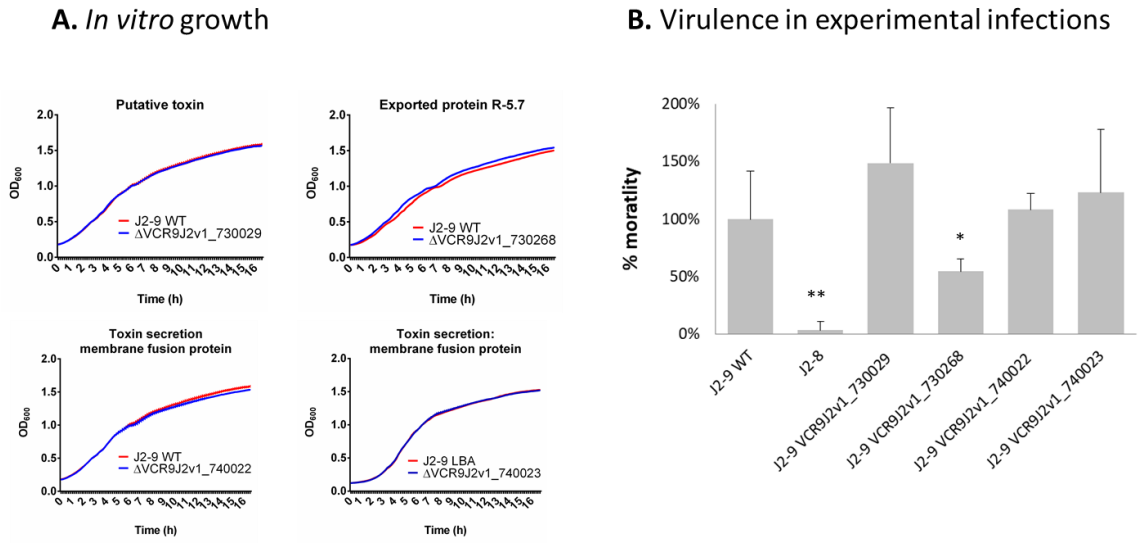

Figure S9 | Phenotyping of *V. crassostreae* J2-9 mutants.

A. Growth curves of wild-type J2-9 and isogenic mutants. Cultures were made in LB NaCl 0.5M. OD_{600} was recorded in triplicate for each strain every 10 minutes after continuous orbital shaking in a TECAN M200 Infinite Pro plate reader, for a 16 hour period at 20°C. B. Virulence in oyster experimental infections. Virulence was assessed by intramuscular injection of juvenile oysters in three independent experiments. J2-8 was used as a negative control. Mortalities were recorded at day 1. Data are expressed as a percentage of the mortality induced by the wild-type strains. Strains or mutants significantly less virulent than the wild-type J2-9 are indicated by asterisks (Kruskal-Wallis test with Dunn's multiple comparison test). *$p<0.05$; **$p<0.01$

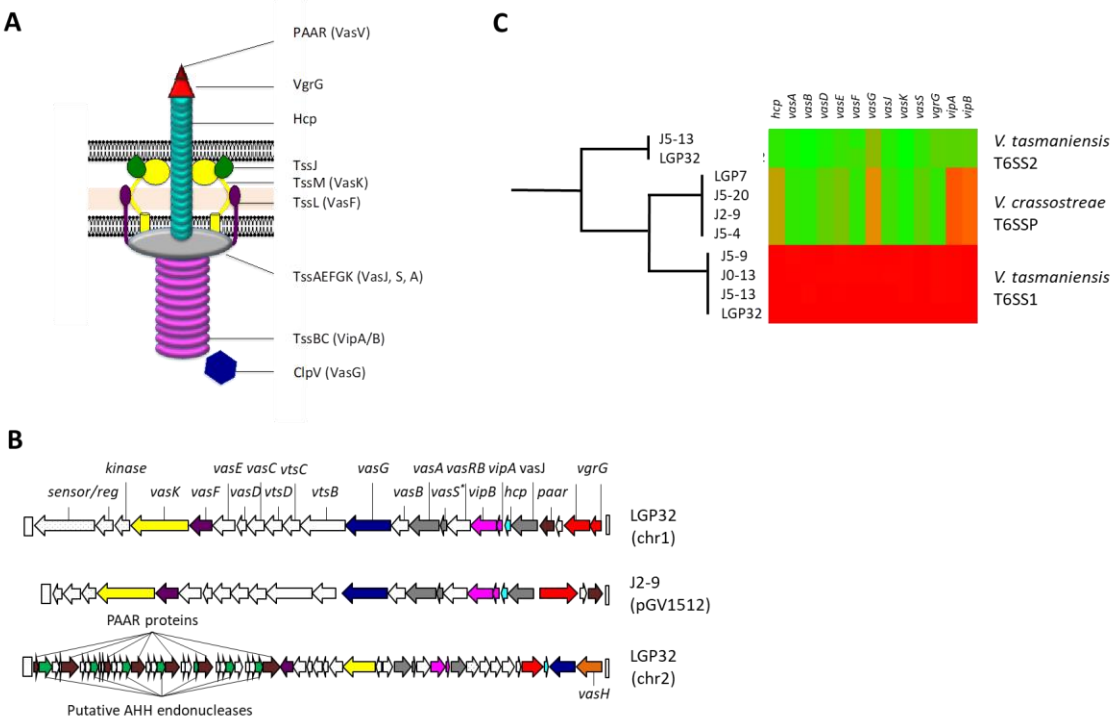

Figure S10 | The type 6 secretion system of *V. tasmaniensis* and *V. crassostreae*.

A. Schematic representation of the assembled T6SS. The core-proteins of the T6SS are colored and named. B. Genes organization of the two T6SS of *V. tasmaniensis* LGP32 (chr1 : chromosome 1 ; chr2 : chromosome 2) and the T6SS of *V. crassostreae* J2-9 localized on a plasmid (pGV1512). The genes are named and colored in accordance to the previously shown schematic structure of the T6SS. C. Conservation of the core-proteins of the T6SSs in multiple strains of *V. tasmaniensis* and *V. crassostreae*.

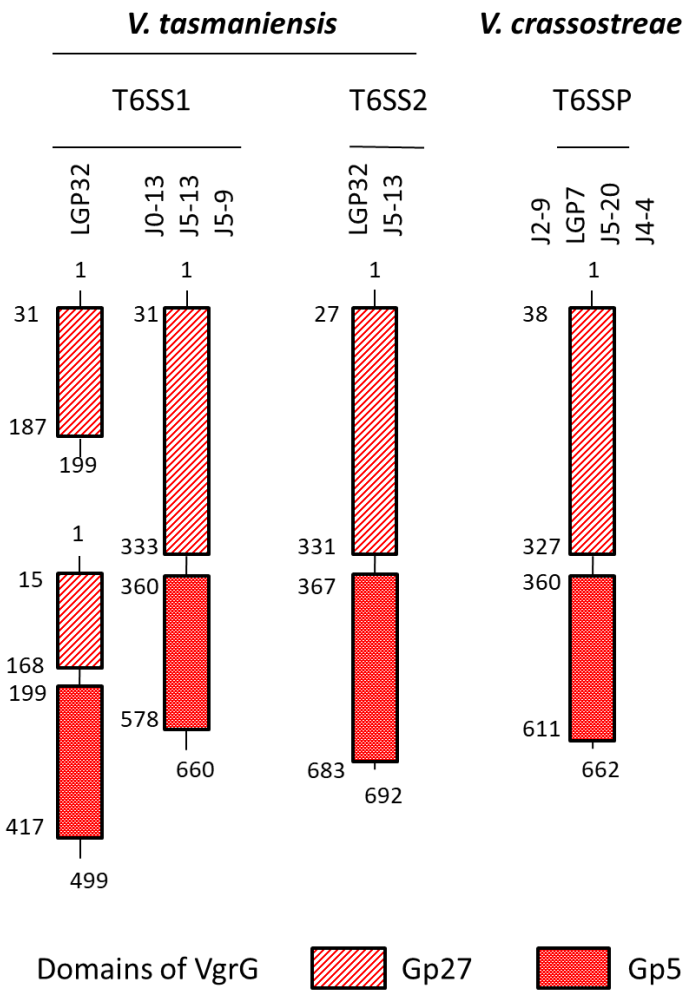

Figure S11 l Functional annotation of VgrG in the T6SSs of *V. tasmaniensis* and *V. crassostreae*.

The different domains are indicated by squared with different motifs. The numbers indicate the beginning/end of the different domains.

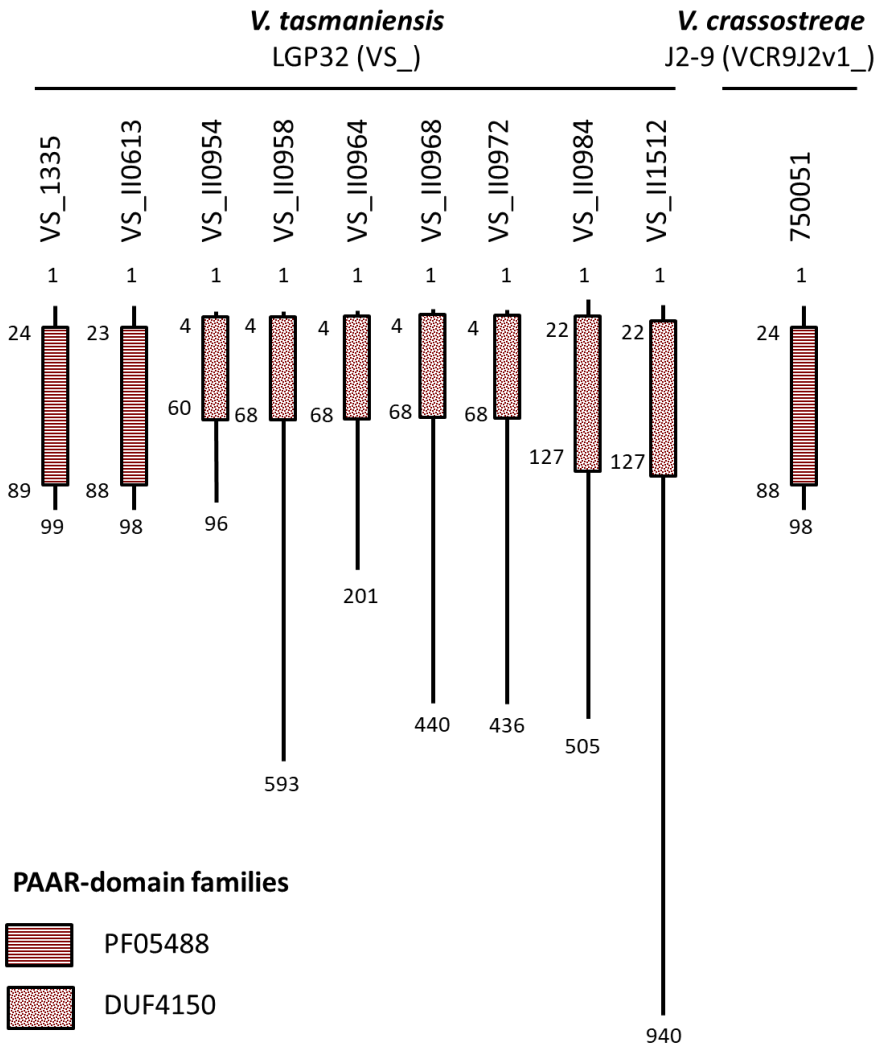

Figure S12 l Functional annotation of PAAR in the T6SSs of *V. tasmaniensis* and *V. crassostreae*.

The different domains are indicated by squared with different motifs. The numbers indicate the beginning/end of the different domains.

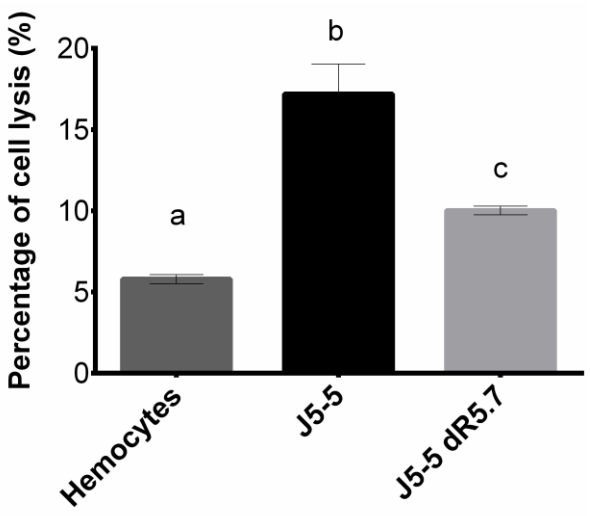

Figure S13 l Cytotoxicity of *V. crassostreae* J5-5 wild-type and isogenic mutant lacking the R5.7 virulence gene.

Cytotoxicity was determined on monolayers of hemocytes and monitored by the Sytox green assay. Cells were infected with bacteria at a MOI of 50:1. Maximum of cytotoxicity of vibrios is displayed. Error bars represent the standard deviation of the mean (RM-ANOVA p-value<0.001).

Table S1 | qPCR quantification of vibrios in oyster tissues.
Real-time qPCR was performed on 40ng/µl of DNA on the same samples using for RNAseq. Quantification of vibrios was calculated in number of vibrio genome copy per number of oyster genome copy because of Avogadro number and genome size of oyster and vibrios. These primers have been chosen because they are specific for each vibrio species. The ratio is the mean of 3 independent experiments.

Strains	Ratio: copy of vibrio genome/copy of oyster genome	Standard deviation
LGP32	0.045	0.037
LMG20 012T	0.015	0.005
J2-9	0.02	0.0014
J2-8	0.02	0.0038

Table S2. Bacterial strains

Strain	Description	Mutated gene	Reference
Π3813	*lacIQ, thi1, supE44, endA1, recA1, hsdR17, gyrA462, zei298::Tn10*, *DthyA::(erm-pir116)* [Tc^R Erm ^{R}]		Le Roux et al., 2007
β3914	(F $^-$) RP4-2-Tc::Mu ΔdapA ::*(erm-pir116), gyrA462, zei298::Tn10* [Km^R Em^R Tc^R]		Le Roux et al., 2007
GV1508	J2-9, *V. crassostreae*		Lemire et al., 2015
GV1476	J2-9 + pMRB-P_{LAC}*gfp*		Bruto et al., 2017
GV1438	J2-9 *ΔpGV1512*		Bruto et al., 2017
GV1023	J2-9 *ΔR5.7*	VCR9J2v1_730268	Lemire et al., 2015
	J2-9 Δ*VCR9J2v1_740022::pSW23T* [Cm^R]	VCR9J2v1_740022	This study
	J2-9 Δ*VCR9J2v1_740023::pSW23T* [Cm^R]	VCR9J2v1_740023	This study
	J2-9 Δ*VCR9J2v1_730029::pSW23T* [Cm^R]	VCR9J2v1_730029	This study
GV1460	J2-8, *Vibrio sp.*		Lemire et al., 2015
GV1470	J2-8 + pMRB-P_{LAC}*gfp*		Bruto et al., 2017
	J5-4, *V. crassostreae*		Lemire et al., 2015
	J5-5, *V. crassostreae*		Lemire et al., 2015
GV1026	J5-5 *ΔR5.7*		Lemire et al., 2015
	J5-20, *V. crassostreae*		Lemire et al., 2015
	LGP8, *V. crassostreae*		Faury et al., 2005
	LGP32, *V. tasmaniensis*		Gay et al., 2004
	LGP32 + pMRB-P_{LAC}*gfp*		Vanhove et al., 2016
	LGP32 Δ*vipA T6SS1::pSW23T* [Cm^R]	VS_1332	This study
	LGP32 Δ*vipA T6SS2::pSW23T* [Cm^R]	VS_II0997	This study
	LGP32 Δ*mshM::pSW23T* [Cm^R]	VS_0329	This study
	LGP32 Δ*pilB::pSW23T* [Cm^R]	VS_2548	This study
	LGP32 Δ*rtx::pSW23T* [Cm^R]	VS_1394	This study
GV76	LGP32 Δ*rtx1*	VS_II0512	Binesse et al., 2008

J0-13, *V. tasmaniensis*	Lemire et al., 2015
J5-13, *V. tasmaniensis*	Lemire et al., 2016
J5-9, *V. tasmaniensis*	Lemire et al., 2017
LMG20012T, *V. tasmaniensis*	Thompson et al., 2003
LMG20012T + pMRB-P_{LAC}*gfp*	Vanhove et al., 2016

Table S3. Plasmids

Plasmid	Description	Reference
pSW23T	$oriV_{R6K}$; $oriT_{RP4;}$ [Cm^R]	Demarre et al. 2005
pSWδVCR9J2v1_740022	pSW23T; *ΔVCR9J2v1_740022*	This study
pSWδVCR9J2v1_740023	pSW23T; *ΔVCR9J2v1_740023*	This study
pSWδVCR9J2v1_730029	pSW23T; *ΔVCR9J2v1_730029*	This study
pSWδmshM	pSW23T; *ΔmshM VS_0329*	This study
pSWδpilB	pSW23T; *ΔpilB VS_2548*	This study
pSWδrtx	pSW23T; *Δrtx VS_1394*	This study
pSWδvipAT6SS1T	pSW23T; *ΔvipA T6SS1*	This study
pSWδvipAT6SS2T	pSW23T; *ΔvipA T6SS2*	This study
pMRB-P_{LAC}*gfp*	$oriV_{R6Kg}$; $oriT_{RP4}$; $oriV_{pB1067;}$ P_{LAC}- *gfp* [Cm^R]	Le Roux et al., 2011

Table S4. Oligonucleotides

Oligonucleotide	Gene id	Sequence 5'-3'	Description	Organism	Use
CGI_10007949 F1	CGI_10007949	GGATGACGTGTTTCGTAGGG	B-1,3-galactosyltransferase brn	*C. gigas*	qRT-PCR of host genes
CGI_10007949 R1	CGI_10007949	TCAATGTCTGCCAACAGCTC	B-1,3-galactosyltransferase brn	*C. gigas*	qRT-PCR of host genes
CGI_10010688 F2	CGI_10010688	GACGGAAAGCTGGACACTGA	Bone-morphogenetic 1-like	*C. gigas*	qRT-PCR of host genes
CGI_10010688 R2	CGI_10010688	AGGTCATAGGGAGGGGCTTT	Bone-morphogenetic 1-like	*C. gigas*	qRT-PCR of host genes
CGI_10000441 F2	CGI_10000441	CCCAGGGTGCTCAACAATCA	Krueppel-like factor 5	*C. gigas*	qRT-PCR of host genes
CGI_10000441 R2	CGI_10000441	TGTGTTTTCGTATGTGGCGC	Krueppel-like factor 5	*C. gigas*	qRT-PCR of host genes
CGI_10000066 F2	CGI_10000066	TCTGCTCTGATTCGTGTCCA	Metallothionein	*C. gigas*	qRT-PCR of host genes
CGI_10000066 R2	CGI_10000066	TTGCAGTTTTCCGGTCCAGT	Metallothionein	*C. gigas*	qRT-PCR of host genes
CGI_10024165 F2	CGI_10024165	AGGATGAGACGGTTGCTCAG	Paired bov Pax-8-like isoform X1	*C. gigas*	qRT-PCR of host genes
CGI_10024165 R2	CGI_10024165	CCAACAACTTTGGCAGAACC	Paired bov Pax-8-like isoform X1	*C. gigas*	qRT-PCR of host genes
CGI_10020521 F1	CGI_10020521	CCACCTACACTCCAACGGAC	Zinc transporter 2-like	*C. gigas*	qRT-PCR of host genes

CGI_10020521R1	CGI_10020521	GGACGTGGATAAAGGCTGCT	Zinc transporter 2-like	*C. gigas*	qRT-PCR of host genes
CGI_10003627F1	CGI_10003627	AGATTGCCTGTCCAGTCACG	Metalloreductas STEAP4-like	*C. gigas*	qRT-PCR of host genes
CGI_10003627R1	CGI_10003627	AAACTTCATGGCTCCCTCCG	Metalloreductas STEAP4-like	*C. gigas*	qRT-PCR of host genes
CGI_10002304F1	CGI_10002304	TGTATCCGGTCGAGAGTGAG	Cyclin-G-associated kinase-like	*C. gigas*	qRT-PCR of host genes
CGI_10002304R1	CGI_10002304	TAACCGATTCCAGCTTGCGG	Cyclin-G-associated kinase-like	*C. gigas*	qRT-PCR of host genes
CGI_10010647F2	CGI_10010647	TACGTCGCCTTCACAGACAC	Heat shock 70	*C. gigas*	qRT-PCR of host genes
CGI_10010647R2	CGI_10010647	CGGCCAATGTTTCATGTCGG	Heat shock 70	*C. gigas*	qRT-PCR of host genes
CGI_10019038F2	CGI_10019038	TGGCCACATTGTCCCTTCAG	Arginine deiminase/G1/S-specific cyclin-E1	*C. gigas*	qRT-PCR of host genes
CGI_10019038 R2	CGI_10019038	CGAAGGACCAGTTGAGGAGG	Arginine deiminase/G1/S-specific cyclin-E1	*C. gigas*	qRT-PCR of host genes
CGI_10025754 F1	CGI_10025754	GCCCACGAATCTTGCTGAAC	Interleukin 17	*C. gigas*	qRT-PCR of host genes
CGI_10025754 R1	CGI_10025754	TTTGGGTAGCGGGTGGAAAG	Interleukin 17	*C. gigas*	qRT-PCR of host genes
CGI_10000478 F1	CGI_10000478	GACGACCCTATCCCAACACC	Neuronal acethylcholine receptor subunit α-6-like	*C. gigas*	qRT-PCR of host genes
CGI_10000478 R1	CGI_10000478	ATCTCGCCGATCCTTTTCCC	Neuronal acethylcholine receptor	*C. gigas*	qRT-PCR of host

			subunit α-6-like		genes
CGI_10004930 F2	CGI_10004930	AAGTGGTCGAGAAACACCCG	NADPH oxidase 5	*C. gigas*	qRT-PCR of host genes
CGI_10004930 R2	CGI_10004930	CCGGGTCAGACGAACTCTTC	NADPH oxidase 5	*C. gigas*	qRT-PCR of host genes
CGI_10007268 F2	CGI_10007268	AGCAATGCTGGACACAACAG	Zinc transporter ZIP10-like isoform X1	*C. gigas*	qRT-PCR of host genes
CGI_10007268 R2	CGI_10007268	AATGGCGATGAAGCTGTACC	Zinc transporter ZIP10-like isoform X1	*C. gigas*	qRT-PCR of host genes
CGI_10009274 F2	CGI_10009274	AGCTGACAACACTGCCCAAT	Complement C1q tumor necrosis factor-related 7-like	*C. gigas*	qRT-PCR of host genes
CGI_10009274 R2	CGI_10009274	TTACTGGTTTCAGCTGTGCG	Complement C1q tumor necrosis factor-related 7-like	*C. gigas*	qRT-PCR of host genes
CGI_10000910 F2	CGI_10000910	AATGTCACAATGGGAAGCGC	Complement C1q4	*C. gigas*	qRT-PCR of host genes
CGI_10000910 R2	CGI_10000910	GGAGGTGGAATATGCGCTGT	Complement C1q4	*C. gigas*	qRT-PCR of host genes
CGI_10020815 F2	CGI_10020815	TGGCCAACATGAACATGTCC	Complement C1q2	*C. gigas*	qRT-PCR of host genes
CGI_10020815 R2	CGI_10020815	TGCTCCCACTGTTGTACCAA	Complement C1q2	*C. gigas*	qRT-PCR of host genes
CGI_10000960 F1	CGI_10000960	ACTGGGGAAAGAGGACGGAT	Frizzled-1	*C. gigas*	qRT-PCR of host genes
CGI_10000960 R1	CGI_10000960	ACACGCTTGGCTCCATGTAA	Frizzled-1	*C. gigas*	qRT-PCR of host genes

CGI_10020472 F2	CGI_10020472	TGATGGACTCGGCTCAGTTG	Deleted in malignant brain tumors 1-like	*C. gigas*	qRT-PCR of host genes
CGI_10020472 R2	CGI_10020472	TCAATGGCGGTTCTCTCACC	Deleted in malignant brain tumors 1-like	*C. gigas*	qRT-PCR of host genes
EFUfw	AB122066	GAGCGTGAACGTGGTATCAC	EF1	*C. gigas*	qRT-PCR of host genes
EFUrv	AB122066	ACAGCACAGTCAGCCTGTGA	EF1	*C. gigas*	qRT-PCR of host genes
C23fw	HS119070	AATCTTGCACCGTCATGCAG	C23	*C. gigas*	qRT-PCR of host genes
C23rv	HS119070	AATCAATCTCTGCTGATCTGC	C23	*C. gigas*	qRT-PCR of host genes
rp56F	FP004478	CAGAAGTGCCAGCTGACAGTC	RP56	*C. gigas*	qRT-PCR of host genes
rp56R	FP004478	AGAAGCAATCTCACACGGAC	RP56	*C. gigas*	qRT-PCR of host genes
OmpUS3	VS_2494	GTCCTACAGACAGCGATAGC	Porin OmpU	*V. tasmaniensis* LGP32	qPCR quantification of vibrios
OmpUAS2	VS_2494	GTGGTAAGCCATGATATCGC	Porin OmpU	*V. tasmaniensis* LGP32	qPCR quantification of vibrios
R5-2aF	VRSK9J2v1_730268	GGATGGGACCAACTACGGTG	Protein R5-2	*V. crassostreae* J2-9	qPCR quantification of vibrios

R5-2aR	VRSK9J2v1_730268	CGTAGCCCGGAGGAAGAATC	Protein R5-2	*V. crassostreae* J2-9	qPCR quantification of vibrios
LMG20012TF2	VTAS012-v1-10089	GGCGTTTCTTCACTTGCGAC	Exported protein of unknow function	*V. tasmaniensis* LMG20 012T	qPCR quantification of vibrios
LMG20012TR2	VTAS012-v1-10089	TTTGCGGAGAAGTGCTAGGG	Exported protein of unknow function	*V. tasmaniensis* LMG20 012T	qPCR quantification of vibrios
J2-8F2	VCR8J2v1-840028	GAGCTTGAGATGGAGAATCG	Anticodon nuclease	Vibrio sp. J2-8	qPCR quantification of vibrios
J2-8R2	VCR8J2v1-840028	ACCGTTTCTACTTCTGCACC	Anticodon nuclease	Vibrio sp. J2-8	qPCR quantification of vibrios
ΔmshM-1	VS_0329	CGGCGTTAGAAATGGGTGAG	MSHA biogenesis protein MshM	*V. tasmaniensis* LGP32	Mutagenesis
ΔmshM-2	VS_0329	CCAAAGAAGAGCGCCAGATC	MSHA biogenesis protein MshM	*V. tasmaniensis* LGP32	Mutagenesis
ΔpilB-1	VS_2548	GCCTGACTCAAGAACAAGCC	Type IV pilin assembly protein ATPase PilB	*V. tasmaniensis* LGP32	Mutagenesis
ΔpilB-2	VS_2548	GATTGGCGAGCTCATCTTGG	Type IV pilin assembly protein ATPase PilB	*V. tasmaniensis* LGP32	Mutagenesis
Δrtx-1	VS_1394	TCAAAGTCCATGATGCTGCG	Putative hemolysin-type RTX toxin	*V. tasmaniensis* LGP32	Mutagenesis

Δrtx-2	VS_1394	CAAGGTTTGCTTTGCCAACG	Putative hemolysin-type RTX toxin	*V. tasmaniensis* LGP32	Mutagenesis
ΔVCR9J2v1_730029-1	VCR9J2v1_730029	CCAATGGTTGGCGCTACTCC	Putative NAD(+)—arginine ADP ribosyltransferase	*V. crassostreae* J2-9	Mutagenesis
ΔVCR9J2v1_730029-2	VCR9J2v1_730029	CGCTCTATCTGGGTGATTCG	Putative NAD(+)—arginine ADP ribosyltransferase	*V. crassostreae* J2-9	Mutagenesis
ΔVCR9J2v1_740022-1	VCR9J2v1_740022	TGAGTTCGCTTCAGGTCGAG	Toxin secretion: membrane fusion protein (fragment)	*V. crassostreae* J2-9	Mutagenesis
ΔVCR9J2v1_740022-2	VCR9J2v1_740022	TAA CCA TTC TAG GAG CGT GC	Toxin secretion: membrane fusion protein (fragment)	*V. crassostreae* J2-9	Mutagenesis
ΔVCR9J2v1_740023-1	VCR9J2v1_740023	AACGCTAACAGGTCGCGTCG	Toxin secretion: membrane fusion protein (fragment)	*V. crassostreae* J2-9	Mutagenesis
ΔVCR9J2v1_740023-2	VCR9J2v1_740023	GTCAAGGCGTATGGTGTTGG	Toxin secretion: membrane fusion protein (fragment)	*V. crassostreae* J2-9	Mutagenesis
ΔvipAT6SS1-1	VS_1332	GtatcgataagcttgatatcgaattcTGAC GTTGAGACTAATGGCG	VipA protein from T6SS1	*V. tasmaniensis* LGP32	Mutagenesis
ΔvipAT6SS1-2	VS_1332	CccccgggctgcaggaattcTCGTGTCT GCACTTTGTAGAAC	VipA protein from T6SS1	*V. tasmaniensis* LGP32	Mutagenesis
ΔvipAT6SS2-1	VS_II0997	GtatcgataagcttgatatcgaattcTTCC AGCGACAGGCGATGCG	VipA protein from T6SS2	*V. tasmaniensis* LGP32	Mutagenesis
ΔvipAT6SS2-2	VS_II0997	CccccgggctgcaggaattcTCTTCATC TTGAAGAACAGCTGC	VipA protein from T6SS2	*V. tasmaniensis* LGP32	Mutagenesis
Ext mshM-1	VS_0329	ATGTATCAAGCTCACTTTAG	MSHA biogenesis protein MshM	*V. tasmaniensis* LGP32	Control of mutagenesis
Ext mshM-2	VS_0329	CCAACCCCACAGCATTGGCG	MSHA biogenesis protein MshM	*V. tasmaniensis*	Control of

				LGP32	mutagenesis
Ext pilB-1	VS_2548	GTGTGTAGTGCTAACCAACC	Type IV pilin assembly protein ATPase PilB	*V. tasmaniensis* LGP32	Control of mutagenesis
Ext pilB-2	VS_2548	AGGGCATTGAGATAGAGCGC	Type IV pilin assembly protein ATPase PilB	*V. tasmaniensis* LGP32	Control of mutagenesis
Ext rtx-1	VS_1394	GAAAGATGCCCAAGGTAACG	Putative hemolysin-type RTX toxin	*V. tasmaniensis* LGP32	Control of mutagenesis
Ext rtx-2	VS_1394	ACTCAGTTTAACGCCATCCG	Putative hemolysin-type RTX toxin	*V. tasmaniensis* LGP32	Control of mutagenesis
Ext VCR9J2v1_730029-1	VCR9J2v1_730029	GTTGTCTGAGCTTTACTGCC	Putative NAD(+)—arginine ADP ribosyltransferase	*V. crassostreae* J2-9	Control of mutagenesis
Ext VCR9J2v1_730029-2	VCR9J2v1_730029	TGTACAAACGAGAGAGTGCC	Putative NAD(+)—arginine ADP ribosyltransferase	*V. crassostreae* J2-9	Control of mutagenesis
Ext VCR9J2v1_740022-1	VCR9J2v1_740022	AAGCTGGCTTTTTAGTACGG	Toxin secretion: membrane fusion protein (fragment	*V. crassostreae* J2-9	Control of mutagenesis
Ext VCR9J2v1_740022-2	VCR9J2v1_740022	AGCTCTGGGTAGAGGAAGG	Toxin secretion: membrane fusion protein (fragment	*V. crassostreae* J2-9	Control of mutagenesis
Ext VCR9J2v1_740023-1	VCR9J2v1_740023	ATGTTATTTCGCCGACAAGTTC	Toxin secretion: membrane fusion protein (fragment	*V. crassostreae* J2-9	Control of mutagenesis
Ext VCR9J2v1_740023-2	VCR9J2v1_740023	TTATTCGCTTCTTGGTATTC	Toxin secretion: membrane fusion protein (fragment	*V. crassostreae* J2-9	Control of mutagenesis
Ext vipAT6SS1-1	VS_1332	ACGCGTAAGTAAGAACCGCG	VipA protein from T6SS1	*V. tasmaniensis* LGP32	Control of mutagenesis
Ext vipAT6SS1-2	VS_1332	CCTAGCTCATCAGAAAGCGC	VipA protein from T6SS1	*V. tasmaniensis* LGP32	Control of mutagenesis

Ext vipAT6SS2-1	VS_II0997	TGATGGCTCGGTGGCTCCG	VipA protein from T6SS2	*V. tasmaniensis* LGP32	Control of mutagenesis
Ext vipAT6SS2-2	VS_II0997	TCGCCTTGGTCTGCACCAATG	VipA protein from T6SS2	*V. tasmaniensis* LGP32	Control of mutagenesis
vipA1-F	VS_1332	GGTGATGACAGCCAGTTTGA	VipA protein from T6SS1	*V. tasmaniensis* LGP32	qRT-PCR of bacterial genes
vipA1-R	VS_1332	CGAGAACGATCGGCTTTAGA	VipA protein from T6SS1	*V. tasmaniensis* LGP32	qRT-PCR of bacterial genes
vipA2-F	VS_II0997	GCCTTGGTTGCATTAAAAGG	VipA protein from T6SS2	*V. tasmaniensis* LGP32	qRT-PCR of bacterial genes
vipA2-R	VS_II0997	TGGTCTGCACCAATGCTAAG	VipA protein from T6SS2	*V. tasmaniensis* LGP32	qRT-PCR of bacterial genes
6PKF-F	VS_2913	GCCGTCACTGTGGTGACCTT	6-phosphofructokinase	*V. tasmaniensis* LGP32	qRT-PCR of bacterial genes
6PKF-R	VS_2913	TGCTTCTTGCCTTTCGCAAT	6-phosphofructokinase	*V. tasmaniensis* LGP32	qRT-PCR of bacterial genes
MGS-F	VS_II1055	CTTTATGCAACGGGCACGAC	Methyl glyoxal synthase	*V. tasmaniensis* LGP32	qRT-PCR of bacterial genes
MGS-R	VS_II1055	GGTCGTGTGGTACGGCATTTA	Methyl glyoxal synthase	*V. tasmaniensis* LGP32	qRT-PCR of bacterial genes

References

1. Gay M, Berthe FC, & Le Roux F (2004) Screening of Vibrio isolates to develop an experimental infection model in the Pacific oyster Crassostrea gigas. (Translated from eng) *Dis Aquat Organ* 59(1):49-56 (in eng).
2. Lemire A, *et al.* (2015) Populations, not clones, are the unit of vibrio pathogenesis in naturally infected oysters. (Translated from English) *Isme Journal* 9(7):1523-1531 (in English).
3. Thompson FL, Thompson CC, & Swings J (2003) Vibrio tasmaniensis sp. nov., isolated from Atlantic salmon (Salmo salar L.). (Translated from eng) *Syst Appl Microbiol* 26(1):65-69 (in eng).
4. de Lorgeril J, *et al.* (2018) Immune-suppression by OsHV-1 viral infection causes fatal bacteraemia in Pacific oysters. (Translated from eng) *Nat Commun* 9(1):4215 (in eng).
5. Petton B, Pernet F, Robert R, & Boudry P (2013) Temperature influence on pathogen transmission and subsequent mortalities in juvenile Pacific oysters Crassostrea gigas. (Translated from English) *Aquaculture Environment Interactions* 3(3):257-273 (in English).
6. Duperthuy M, *et al.* (2010) The major outer membrane protein OmpU of Vibrio splendidus contributes to host antimicrobial peptide resistance and is required for virulence in the oyster Crassostrea gigas. (Translated from eng) *Environ Microbiol* 12(4):951-963 (in eng).
7. Suquet M, *et al.* (2009) Anesthesia in Pacific oyster, Crassostrea gigas. *Aquat. Living Resour.* 22 29-34.
8. Le Roux F, Binesse J, Saulnier D, & Mazel D (2007) Construction of a Vibrio splendidus mutant lacking the metalloprotease gene vsm by use of a novel counterselectable suicide vector. (Translated from eng) *Appl Environ Microbiol* 73(3):777-784 (in eng).
9. Le Roux F, Davis BM, & Waldor MK (2011) Conserved small RNAs govern replication and incompatibility of a diverse new plasmid family from marine bacteria. (Translated from eng) *Nucleic Acids Res* 39(3):1004-1013 (in eng).
10. Demarre G, *et al.* (2005) A new family of mobilizable suicide plasmids based on broad host range R388 plasmid (IncW) and RP4 plasmid (IncPalpha) conjugative machineries and their cognate Escherichia coli host strains. (Translated from eng) *Res Microbiol* 156(2):245-255 (in eng).
11. Le Roux F, *et al.* (2009) Genome sequence of Vibrio splendidus: an abundant planctonic marine species with a large genotypic diversity. (Translated from eng) *Environ Microbiol* 11(8):1959-1970 (in eng).
12. Afgan E, *et al.* (2018) The Galaxy platform for accessible, reproducible and collaborative biomedical analyses: 2018 update. (Translated from eng) *Nucleic Acids Res* 46(W1):W537-W544 (in eng).
13. Zhang G, *et al.* (2012) The oyster genome reveals stress adaptation and complexity of shell formation. (Translated from eng) *Nature* 490(7418):49-54 (in eng).
14. Dobin A, *et al.* (2013) STAR: ultrafast universal RNA-seq aligner. (Translated from eng) *Bioinformatics* 29(1):15-21 (in eng).
15. Anders S, Pyl PT, & Huber W (2015) HTSeq--a Python framework to work with high-throughput sequencing data. (Translated from eng) *Bioinformatics* 31(2):166-169 (in eng).

16. Love MI, Huber W, & Anders S (2014) Moderated estimation of fold change and dispersion for RNA-seq data with DESeq2. (Translated from eng) *Genome Biol* 15(12):550 (in eng).
17. Buchfink B, Xie C, & Huson DH (2015) Fast and sensitive protein alignment using DIAMOND. (Translated from eng) *Nat Methods* 12(1):59-60 (in eng).
18. Bolger AM, Lohse M, & Usadel B (2014) Trimmomatic: a flexible trimmer for Illumina sequence data. (Translated from eng) *Bioinformatics* 30(15):2114-2120 (in eng).
19. Langmead B & Salzberg SL (2012) Fast gapped-read alignment with Bowtie 2. (Translated from eng) *Nat Methods* 9(4):357-359 (in eng).
20. Liao Y, Smyth GK, & Shi W (2014) featureCounts: an efficient general purpose program for assigning sequence reads to genomic features. (Translated from eng) *Bioinformatics* 30(7):923-930 (in eng).
21. Altschul SF, Gish W, Miller W, Myers EW, & Lipman DJ (1990) Basic local alignment search tool. (Translated from eng) *J Mol Biol* 215(3):403-410 (in eng).
22. Conesa A, *et al.* (2005) Blast2GO: a universal tool for annotation, visualization and analysis in functional genomics research. (Translated from eng) *Bioinformatics* 21(18):3674-3676 (in eng).
23. Medigue C, *et al.* (2017) MicroScope-an integrated resource for community expertise of gene functions and comparative analysis of microbial genomic and metabolic data. (Translated from eng) *Brief Bioinform* (in eng).
24. Caspi R, *et al.* (2018) The MetaCyc database of metabolic pathways and enzymes. (Translated from eng) *Nucleic Acids Res* 46(D1):D633-D639 (in eng).
25. Vallenet D, *et al.* (2013) MicroScope--an integrated microbial resource for the curation and comparative analysis of genomic and metabolic data. (Translated from eng) *Nucleic Acids Res* 41(Database issue):D636-647 (in eng).